

Crystal structure of synthesized $\text{CuGa}_{0.5}\text{In}_{0.5}\text{Te}_2$ determined by X-ray powder diffraction using the Rietveld method

M. LEÓN, J. M. MERINO, J. L. MARTÍN DE VIDALES*

*Departamento de Física Aplicada. Facultad de Ciencias, C-XII, and *Facultad de Ciencias, C-VI, Universidad Autónoma de Madrid, 28049 Madrid, Spain*

A full profile X-ray powder diffraction structure refinement has been carried out on a sample of synthesized $\text{CuGa}_{0.5}\text{In}_{0.5}\text{Te}_2$ using graphite monochromatized $\text{CuK}\alpha$ step-scan data and a profile shape of the Pearson VII type. The most satisfactory convergence was achieved at $R_p = 0.0483$, $R_{wp} = 0.0641$, $R_B = 0.0208$ and $R_F = 0.0320$, where, R is the Rietveld refinement. The derived structural parameters at 26°C are $a = 0.610\,09(2)$ nm, $c = 1.219\,79(4)$ nm and $x[\text{Te}] = 0.2279(3)$. The ratio between lattice parameters, $\eta = c/2a = 0.9997(0)$ differed very slightly from 1, while the non-ideal anion displacements, $x[\text{Te}] \neq 1/4$, was manifested by the existence of bond alternation of Cu–Te, Ga–Te and In–Te.

1. Introduction

The ternary compounds ABC_2 ($A = \text{Cu}$ and Ag ; $B = \text{Al}$, Ga and In ; $C = \text{S}$, Se and Te) belong to the I–III–VI₂ semiconducting materials which crystallize in the tetragonal chalcopyrite structure with space group D_{2d}^{12} I42d. Each anion (C) is tetrahedrally coordinated by two A and two B cations, while each cation is tetrahedrally coordinated by four anions [1]. This ordering gives rise to some interesting anomalies, relative to their binary analogues zinc-blende lattices. First, these compounds often show a tetragonal distortion where the ratio between the lattice parameters, $\eta = c/2a$, differ from 1 by as much as 12%. Second, the anions are displaced from zinc-blende sites and they adopt an equilibrium position closer to one pair of cations than to the other, resulting in unequal bond lengths [2].

The broad range of optical band gaps and carrier mobilities offered by ternary ABC_2 semiconductors, as well as their ability to form various solid solutions and to accommodate different dopants, has led to their emergence as technologically significant device materials, including applications in photovoltaic solar cells, light-emitting diodes, infrared detectors and in various nonlinear optical devices [3].

The atomic positions in the tetragonal unit cell of the chalcopyrite family are: four A cations in sites 4a at (0 0 0), four B cations in sites 4b at (0 0 1/2) and eight C anions in sites 8d at (x 1/4 1/8), when the origin is at 4a [4]. The structure then requires three parameters only (excluding thermal vibrations coefficients) to describe the atomic arrangement completely: the unit cell parameters, a and c , and the anion positional coordinate, x , called $x[\text{Te}]$ in this paper. When $x = 1/4$ and $\eta = 1$, the chalcopyrite-type has the ideal structure, with no tetrahedral distortions.

Recently, Haworth and Tomlinson resolved this atomic arrangement for the CuInTe_2 compound [5], calculating the parameters mentioned above; in a previous work, we have refined this structure for the CuGaTe_2 compound [6]. Powder data of $\text{CuGa}_{0.5}\text{In}_{0.5}\text{Te}_2$ compound have been published by Gržeta–Plenković and Šantić [7] which form the basis of the Powder Diffraction File pattern 34-1499 with $a = 0.6107(2)$ nm, $c = 1.2177(7)$ nm and $c/a = 1.9939$, no comparison with theoretical intensity values was made. There is no report of the measurement of anion displacement, $x[\text{Te}]$, to our knowledge. A precise study of a solid solution begins with accurate knowledge about its structural parameters in order to establish the possibilities of this solid solution with the properties mentioned above. In this work we began the crystallographic characterization of the solid solution $\text{CuGa}_{1-x}\text{In}_x\text{Te}_2$ with the intermediate compound $\text{CuGa}_{0.5}\text{In}_{0.5}\text{Te}_2$. As in the case of CuGaTe_2 [6], we continued with the application of full-profile Rietveld-type powder diffraction structure refinements methods with two-wavelength X-ray data obtained from a conventional automatized step-scan diffractometer. In a further work we will study the lattice parameters, in the same way, of two other intermediate compounds (as well as CuInTe_2) and relate these to other structural parameters of the solid solution.

2. Experimental procedure

The difficulties in obtaining single crystals [1] of these compounds led us to attempt the growth of homogeneous polycrystalline samples of $\text{CuGa}_{0.5}\text{In}_{0.5}\text{Te}_2$. Synthesis was carried out in an evacuated silica glass ampoule using elements with 99.999% purity. Heating and cooling cycles are described in Fig. 1. The quartz

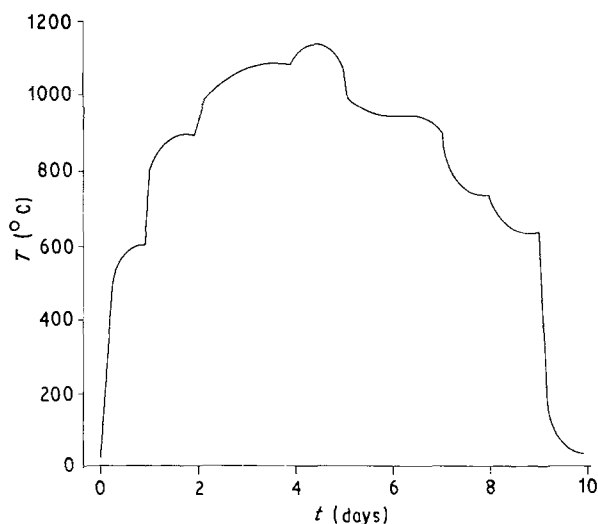


Figure 1 Diagram of the thermal cycle used to synthesize the $\text{CuGa}_{0.5}\text{In}_{0.5}\text{Te}_2$ sample.

tube was heated to 1130°C , avoiding over pressures. The cooling rate was especially low: $5\text{--}10^\circ\text{C h}^{-1}$ across the phase transitions.

Powder diffractometer data were collected with an automatic step-scanning Phillips PW 1080 powder diffraction system. CuK_α ($\lambda = 0.154184\text{ nm}$) radiation was utilized. The divergence slits located in the incident beam were selected to ensure complete illumination of the specimen surface at $12^\circ(2\Theta)$. The powder diffraction pattern was scanned in steps of $0.02^\circ(2\Theta)$ and with a goniometer speed of $1/4^\circ(2\Theta)\text{ min}^{-1}$. At the end of the data collection the stability of the intensity of the incident beam was checked by recording the first lines of the pattern. All the experiment was carried out at a constant temperature of 26.5°C .

These conditions allowed the collection of profile data for a total of 152 Bragg reflections with back-

ground counts in the range 90–160 and a maximum peak intensity of 4265 counts.

To minimize preferred orientation effects due to the layer morphology of the crystallites, the $\text{CuGa}_{0.5}\text{In}_{0.5}\text{Te}_2$ was ground in an agate mortar for $1/4\text{ h}$, and a side-loading method was used to prepare the sample for the diffractometer. Finally, the sample was repacked and rerun three times at $1^\circ(2\Theta)\text{ min}^{-1}$ and $0.02^\circ(2\Theta)$ step-size to check for evidence of preferred orientation. Some changes in the intensity of the 024 peak were noticed among the three data sets, suggesting that preferred orientation effects can be relatively high according to this hkl -vector direction.

3. Structure refinement

The least-squares structure refinements were undertaken with the full-profile, Rietveld-type, program DBW3.2S version 8804 [8, 9] locally modified by Schneider [10] for IBM-AT (R) compatible micro-computers.

The observed X-ray powder profile for the $\text{CuGa}_{0.5}\text{In}_{0.5}\text{Te}_2$ sample is plotted in Fig. 2. It is obvious that most of the peaks in the pattern appear relatively sharp (full width at half maximum (FWHM) $< 0.2^\circ$ in all diagrams). A Pearson VII function [11] was used for the representation of the profile. In this powerful function, the parameter m can be refined as a function of 2Θ as

$$m = N_A + N_B/(2\Theta) + N_C/(2\Theta)^2 \quad (1)$$

where the refinable variables are N_A , N_B and N_C .

On the other hand, this program can accept X-ray data obtained from a conventional diffractometer because it allows the simultaneous refinement of two wavelengths (i.e. α_2 and α_1) if their intensity ratio is known (0.5 in the present case). The weight assigned to the intensity observed at each step i in the pattern is

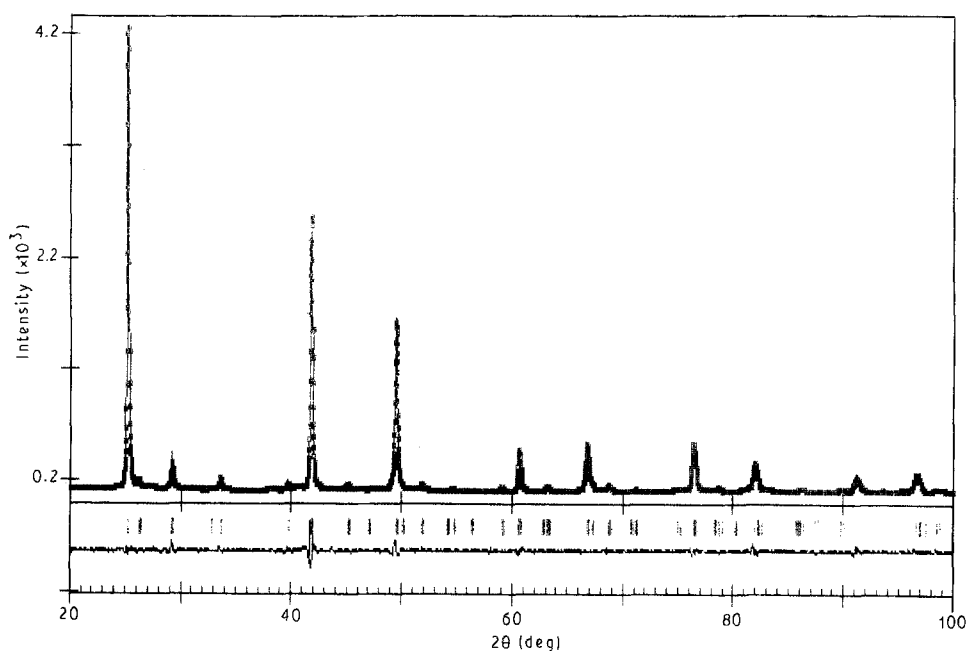


Figure 2 Observed and calculated X-ray diffraction patterns for $\text{CuGa}_{0.5}\text{In}_{0.5}\text{Te}_2$ and the difference between them. The upper trace shows the observed data by dots and the calculated pattern is shown as a solid line. The lower trace is a plot of the difference: observed minus calculated. The vertical markers show positions for the Bragg reflections.

$W_i = 1/Y_{i0}$ and the function minimized in the least-squares procedures is $W_i(Y_{i0} - Y_{ic})^2$, where Y_{i0} and Y_{ic} are the observed and calculated intensities at point i in the pattern including the background intensity points, respectively.

The refined quantities were a C -scale factor, a 2Θ zero shift parameter and the Pearson VII profile shape parameters, N_A , N_B and N_C ; these two last parameters were refined in the final cycles. A peak full width at half maximum (FWHM) function, described by the usual quadratic form in $\text{tg}(\Theta)$

$$\text{FWHM}^2 = U\text{tg}^2\Theta + V\text{tg}\Theta + W \quad (2)$$

where U , V and W are parameters whose values were refined, was calculated for five half-widths on either side of the peak position. The peak asymmetry parameter, P , the unit cell constants, a and c , the x coordinate of the tellurium atom, x [Te], and the isotropic overall thermal parameter, B , were also refined. The background intensity was evaluated in regions without contribution from Bragg reflections, and linear interpolation of these values led to the background correction. The last variable to be refined was the preferred-orientation factor, G_1 .

The refinements were initiated using $a = 0.60000$ nm, $c = 1.19000$ nm, $x = 0.2500$, $N_A = 1.4$, $N_B = N_C = 0.0$, $B_{\text{overall}} = 0.5 \times 10^{-2}$ nm² and a scale factor and a half-width parameters ($U = V = 0$ and $W = 0.04$), estimated by inspection of the observed diffraction pattern. The complete set of results for the best-fit model are given in Table I. A plot of the observed, calculated and difference profiles for the final Rietveld refinement is given in Fig. 2; a list of observed and calculated integrated peak intensities is given in Table II.

TABLE I Final Rietveld refinement parameters for CuGa_{0.5}In_{0.5}Te₂

Cell dimensions	$a = 0.61009(2)$ nm $c = 1.21979(4)$ nm $\eta = c/2a = 0.9997(0)$
Volume	$0.45402(5)$ nm ³
Tetrahedral distortion	x [Te] = $0.2279(3)$
Isotropic overall temperature factor (nm ²)	$B_{\text{overall}} = 0.61(3) \times 10^{-2}$
Pearson VII coefficients $m = 1.57(3)$ at $26^\circ(2\Theta)$	$N_A = 5.8(4)$ $N_B = -311(28)$ $N_C = 5204(455)$
Asymmetry parameter	$P = -0.42(3)$
Preferred orientation coeff.	$G_1 = 0.38(1)$
FWHM function parameters	$U = 0.254(4)$ $V = -0.154(4)$ $W = 0.0529(8)$
Zero shift	$-0.0705(4)$
Scale factor	$0.938(7) \times 10^{-7}$
Bragg reflections	$152(2 \times 76)$
Parameters	14
Agreement indices	R_p 0.0483 R_{wp} 0.0641 R -expected 0.0598 R -Bragg 0.0208 R -structure factors 0.0320 Goodness of fit, G_F 1.1490

Values in parenthesis are estimated standard deviations in the last place.

TABLE II Observed and calculated integrated peak intensities and d -spacings for CuGa_{0.5}In_{0.5}Te₂ reflections with intensities greater than 1% of the maximum calculated value

hkl	d (nm)	I_o	I_c
112	0.35220	100.4	100.0
013	0.33834	1.4	1.7
020	0.30504	3.0	2.9
004	0.30495	2.9	2.7
121	0.26626	2.8	2.6
220	0.21570	23.3	23.2
024	0.21566	47.6	47.6
031	0.20059	1.2	1.2
132	0.18394	26.3	25.8
116	0.18390	18.7	18.4
224	0.17610	1.0	1.1
233	0.15622	1.2	1.2
040	0.15252	6.6	6.7
008	0.15247	6.2	6.4
332	0.13996	5.1	5.1
136	0.13994	10.9	10.8
244	0.12453	11.8	11.8
228	0.12451	7.7	7.8
152	0.11741	5.2	4.8
336	0.11740	3.0	2.8
1110	0.11738	4.5	4.2

^a No differentiated intensities in the experimental X-ray diagram before the Rietveld analysis (see Fig. 2).

4. Discussion

4.1. Discrepancy index

The quantities used to estimate the agreement between the observations and the model during the course of the Rietveld refinement can be written as

The profile

$$R_p = \frac{\sum |Y_{i0} - (1/C) Y_{ic}|}{\sum |Y_{i0}|} \quad (3)$$

The weighted profile

$$R_{wp} = \frac{[\sum W_i(Y_{i0} - Y_{ic}/C)^2 / \sum W_i Y_{i0}]^{1/2}}{\sum W_i Y_{i0}} \quad (4)$$

The Bragg

$$R_B = R_I = \frac{\sum |I_o - I_c|}{\sum I_o} \quad (5)$$

The structure factor

$$R_F = \frac{\sum |I_o^{1/2} - I_c^{1/2}|}{\sum I_o^{1/2}} \quad (6)$$

The expected

$$R_{\text{exp}} = R_E = \frac{[(N - P) / \sum W_i Y_{i0}^{1/2}]^{1/2}}{\sum W_i Y_{i0}^{1/2}} \quad (7)$$

The goodness of fit

$$G_F = [R_{wp}/R_{\text{exp}}]^2 \quad (8)$$

The quantity C is the refinable scale factor. The values Y_{i0} and Y_{ic} are the observed and calculated intensities at point i in the pattern including the background intensity points. In this case the number of intensity points is 4001. The observed and calculated integrated Bragg intensities are denoted I_o and I_c , where the observed intensities are calculated by partitioning the raw data in accordance with the calculated intensities of the component peaks. The number of step intensities and parameters refined are denoted N and P , respectively. N is normally the number of step intensities within the integration range of the Bragg reflections.

The quantity minimized in a Rietveld refinement is the weighted profile R_{wp} , but its numerical value may be somewhat misleading. Thus it is not the value of the minimum reached in the weighted profile R -factor but the structure parameter set (R_B and R_F) obtained from the minimum which is of importance. After Rietveld refinement, the obtained agreement indices, $R_B = 0.0208$ and $R_F = 0.0320$ indicate to the same degree of confidence as for a single-crystal refinement, that the $\text{CuGa}_{0.5}\text{In}_{0.5}\text{Te}_2$ structure is correct. Obviously, other criteria must be used together with the agreement indices discussed, to assess accurately the quality of the refined structure. Probably, the most important test of a structure refinement is whether occupancy factors and bond distances and angles make reasonable chemical sense [12].

The 2Θ positions of Bragg reflections obtained after Rietveld refinement are shown in Table II.

4.2. Structural parameters

The refined positional parameter for tellurium, $x [\text{Te}] = 0.2279(3)$, is lower than the value calculated (0.250) with the "CTB plus $\eta = \eta_{\text{tet}}$ rule" deduced by Jaffe and Zunger [2], using Pauling radii. The refined unit cell parameters show the following values: $a = 0.61009(2)$ nm and $c = 1.21979(6)$ nm. These results determined from the profile refinement, even allowing for the tetragonal symmetry and well-crystallized nature of the sample, are unusually precise, moreover being a quarternary compound. This fact seems to indicate the good fit of the Pearson VII function type used in the Rietveld refinement. The interatomic distances and angles resulting from the determined a , c and $x [\text{Te}]$ values are summarized in Table III.

The ideal distances of the bond lengths Te–Cu and Te–III are in both cases $\pm 0.264(2)$ nm calculated from $x [\text{Te}] = 1/4$. As in the CuGaTe_2 [6] system the differences between these bond lengths and the real ones obtained are very close: 0.076 and 0.080 nm for Cu–Te and III–Te distances, respectively. On the other hand, the Te–Cu–Te angles are $110.676(8)^\circ$ and

$107.088(7)^\circ$, very close to the angles obtained for the CuGaTe_2 [6], whereas the Te–III–Te angles are $111.855(8)^\circ$ and $108.293(8)^\circ$, very different from the ideal chalcopyrite-type structure and from the Te–Ga–Te angles in CuGaTe_2 [6]. These results indicate that when one introduces In in CuGaTe_2 , the Cu– Te_4 tetrahedra remain unchanged whereas the III– Te_4 tetrahedra change not only in length, with the obvious result ($R_{\text{In}} > R_{\text{Ga}}$), but also in shape, losing its regularity.

Although the anion positional coordinate is more deviated from the ideal value for the chalcopyrite structure than its value in the CuGaTe_2 compound, the tetragonal distortion is closer to 1, $\eta = 0.9997(0)$, than in CuGaTe_2 [6] and CuInTe_2 [5]. These results could indicate that the structure of $\text{CuGa}_{0.5}\text{In}_{0.5}\text{Te}_2$ has more stability than other compounds belonging to the same solid solution, and its growth could involve fewer difficulties.

Comparing our results with those of Gržeta-Plenković and Šantić [7], we observe a good agreement in the a parameter ($\Delta a = 0.0006$ nm) but not as good in the c parameter ($\Delta c = 0.0023$ nm). These authors reported the maximum intensity to be 100%, for the 220, 204 reflections, and 85% for the 112 reflection, while we observed the maximum intensity for the 112 reflection (Table II) and 70.9 (47.6 + 23.3) for 220, 204 reflections. This disagreement is notably due to the preferred orientation effects along the 220, 204 reflections, which we have avoided in the preparation of sample by using a side-loading method (see Section 2).

5. Conclusion

Synthesis of the quarternary compound has been carried out resulting in a single-phase polycrystalline material.

Assuming chalcopyrite-type structure, the crystal structure has been determined with the same degree of confidence as for a single-crystal refinement ($R_B = 0.0208$, $R_F = 0.0320$).

On comparing the structural results of $\text{CuGa}_{0.5}\text{In}_{0.5}\text{Te}_2$ with our previous structure refinement of CuGaTe_2 , we observe that the Cu– Te_4 tetrahedra remain unchanged in both cells.

TABLE III Bond distances (nm) and angles (deg) for $\text{CuGa}_{0.5}\text{In}_{0.5}\text{Te}_2$

[Ga– Te_4] and [In– Te_4] tetrahedra		
Ga–Te, In–Te	($\times 4$)	0.2722(1) nm
Te–Ga–Te, Te–In–Te	($\times 3$)	$111.855(8)^\circ$
Te–Te	($\times 3$)	0.4508(2) nm
Te–Ga–Te, Te–In–Te	($\times 3$)	$108.293(8)^\circ$
Te–Te	($\times 3$)	0.4127(2) nm
[Cu– Te_4] tetrahedron		
Cu–Te	($\times 4$)	0.2566(1) nm
Te–Cu–Te	($\times 2$)	$110.676(8)^\circ$
Te–Te	($\times 2$)	0.4412(2) nm
Te–Cu–Te	($\times 4$)	$107.088(7)^\circ$
Te–Te	($\times 4$)	0.4221(2) nm

Shortest distance between cations

Cu–Cu = Cu–Ga = Cu–In = Ga–Ga = Ga–In = In–In = 0.43133(1) nm

References

1. J. L. SHAY and J. H. WERNICK, "Ternary Chalcopyrite Semiconductors: Growth, Electronic Properties and Applications". (Pergamon Press, Oxford, 1974).
2. J. E. JAFFE and A. ZUNGER, *Phys. Rev. B* **29** (1984) 1882.
3. *Idem, ibid.* **28** (1983) 5822.
4. H. HAHN, G. FRANK, W. KLINGLER, A. D. MEYER and G. STORGER, *Z. Anorg. Allg. Chem.* **271** (1953) 153.
5. L. I. HAWORTH and R. D. TOMLINSON, *Powder Diff.* **3**(1) (1988) 43.
6. M. LEON, J. M. MERINO and J. L. MARTIN DE VIDALES, *J. Mater. Sci.* **27** (1992) 4495.
7. B. GRŽETA-PLENKOVIĆ and B. ŠANTIĆ, *J. Appl. Crystallogr.* **16** (1983) 576.
8. H. M. RIETVELD, *ibid.* **2** (1969) 65.

9. D. B. WILES, A. SAKTHIVEL and R. A. YOUNG. "User's Guide to the Program DBW3.2S for Rietveld Analysis of X-ray and Neutron Powder Diffraction Patterns (Version 8804)" (School of Physics, Georgia Institute of Technology, Atlanta, 1988).
10. J. SCHNEIDER, in "IUCr. International Workshop on the Rietveld Method" (Petten, 1989) p. 535.
11. R. A. YOUNG and D. B. WILES, *J. Appl. Crystallogr.* **15** (1982) 430.
12. J. E. POST and D. L. BISH, in "X-ray Powder Diffraction", edited by D. K. Smith and R. L. Snyder (Mineralogical Society of America, New York, 1989), p. 277.

*Received 30 April
and accepted 21 October 1992*